Beyond the dynamic density functional theory for steady currents: Application to driven colloidal particles in a channel

P. Tarazona[1] and Umberto Marini Bettolo Marconi[2,a)]
[1]*Departamento de Física Teórica de la Materia Condensada, and Instituto de Ciencia de Materiales Nicolás Cabrera, Universidad Autónoma de Madrid, E-28049 Madrid, Spain*
[2]*Dipartimento di Fisica and Istituto Nazionale di Fisica della Materia, Università di Camerino via Madonna delle Carceri, 62032 Camerino, Italy*

(Received 1 February 2008; accepted 12 March 2008; published online 22 April 2008)

Motivated by recent studies on the dynamics of colloidal solutions in narrow channels, we consider the steady state properties of an assembly of noninteracting particles subject to the action of a traveling potential moving at a constant speed, while the solvent is modeled by a heat bath at rest in the laboratory frame. Here, since the description we propose takes into account the inertia of the colloidal particles, it is necessary to consider the evolution of both positions and momenta and study the governing equation for the one-particle phase-space distribution. First, we derive the asymptotic form of its solutions as an expansion in Hermite polynomials and their generic properties, such as the force and energy balance, and then we particularize our study to the case of an inverted parabolic potential barrier. We numerically obtain the steady state density and temperature profile and show that the expansion is rapidly convergent for large values of the friction constant and small drifting velocities. On the one hand, the present results confirm the previous studies based on the dynamic density functional theory (DDFT): On the other hand, when the friction constant is large, it display effects such as the presence of a wake behind the barrier and a strong inhomogeneity in the temperature field which are beyond the DDFT description. © *2008 American Institute of Physics*. [DOI: 10.1063/1.2904881]

I. INTRODUCTION

In recent years, we have witnessed the emergence of a new branch of applied physics named microfluidics, which is the science of designing, manufacturing devices, and processes that deal with volumes of fluid on the order of nanoliters.[1–5] Microfluidic systems have diverse and widespread potential applications.[6–8] Some examples of systems and processes that might employ this technology include inkjet printers, blood–cell-separation equipment, biochemical assays, chemical synthesis, genetic analysis, drug screening, electrochromatography, surface micromachining, laser ablation, and mechanical micromilling. Not surprisingly, the medical industry has shown keen interest in microfluidics technology.

Such advances in manipulating fluids[9–11] have recently motivated Penna and Tarazona[12] to consider a model representing a simple device to push a dilute solution of colloidal particles along a narrow channel. In particular, they studied the effect of a moving barrier on a system of noninteracting colloidal particles described by overdamped Langevin dynamics. Under the action of the potential barrier shifting at a constant speed, the fluid achieves a steady state, with density distribution and local current following the moving barrier. These authors showed that such a steady state can be conveniently studied within the dynamic density functional theory (DDFT)[13–15] formalism, since the structure of the relevant equations becomes similar to that of the Euler–Lagrange equations describing a fluid at thermodynamic equilibrium.[16]

On the other hand, the present authors in a recent paper,[17] hereafter referred as Ref. 1, have considered how the inertia of the particles may modify the DDFT picture. They assumed that the colloidal particles have inertia, i.e., are governed by a second order stochastic equation. The governing equation for the associated phase-space distribution turns out to be the Kramers equation[18] and represents the evolution of both positions and momenta of the particles. Since such a representation is still too complex and is often redundant, the authors considered a contraction of such a description by rewriting the Kramers equation in terms of the infinite hierarchy of equations for the velocity moments of the phase-space distribution. In Ref. 1 the hierarchy was systematically truncated by means of a multiple time scale technique, which lead to a self-consistent equation involving only the one-body density. This equation is similar to the DDFT equation, but it contains additional terms taking into account the presence of momentum and energy currents. While in Ref. 1, we considered only transient effects, namely, the decay of initial perturbations toward the equilibrium, time independent, and state, in the present work, we illustrate how the inertial dynamics affects the behavior of systems in situations in which a steady state is induced by the presence of an external time-dependent potential. The results of the present paper show pronounced differences with respect to the DDFT study of Penna and Tarazona and, in particular, display an exponential decay in the structure of the density profile behind the barrier which was not predicted by the DDFT. Moreover, we also

[a)]Electronic mail: bettolou@romal.infn.it.

found that the local temperature is nonuniform throughout the system due to the heating produced by the barrier.

We believe that these findings are generic to nonequilibrium systems where the equilibration mechanism provided by the heat bath is not very rapid. We have shown that when the friction is not sufficiently high, the density alone is not sufficient to characterize the steady state of the system, and additional fields are necessary to provide a complete description.

Generally speaking, we believe that the use of the DDFT is justified when the currents are of diffusive character, while in the cases where convective terms are present, it is necessary to include extra terms which describe the transport of momentum and energy.[19,20]

The present paper is organized as follows. In Sec. II, after presenting the model, we give the structure of the general solution of the Kramers equation in the region where the vanishing potential is small. In Sec. III, we specialize the treatment to the case of steady state conditions and explicitly derive the behavior of the phase-space distribution in the region where the traveling potential vanishes. We also derive the relation between the total force exerted by the barrier on the particles and the friction due to the bath. Finally, in Sec. IV, we give explicit numerical solutions of the Kramers equation in the case of an inverted parabolic barrier. We conclude the paper with a short discussion in Sec. V.

II. KRAMERS EQUATION FOR SHIFTING POTENTIAL BARRIERS AND ITS FREE MODES

The problem of the steady states in a fluid, under the action of a shifting external potential, has been considered within the DDF under several conditions and model interactions.[12,21,22] In all these treatments, the inertia of the particles did not play any role. Here, we wish to consider how the inertial effects modify that picture, and to such a purpose, we consider here the simplest case, which could describe a dilute solution of colloidal particles dragged along a narrow channel under the action of a moving potential barrier, modeled by a time-dependent external potential, $V_{\text{ext}}(x,t)=V_{\text{ext}}(x-ct)$, which acts on the colloidal particles but has negligible effects on the solvent. To such a purpose, here, we consider an assembly of noninteracting identical particles of mass m moving in one dimension, and described by the following stochastic dynamics:[23,24]

$$m\frac{d^2x}{dt^2}=-m\gamma\frac{dx}{dt}+f_{\text{ext}}(x-ct)+\xi(t), \tag{1}$$

with a bath providing the particles a friction constant γ, and a thermalizing noise with

$$\langle\xi(t)\xi(s)\rangle=2\gamma mk_BT_o\delta(t-s), \tag{2}$$

at temperature T_o. The external force associated with the traveling potential is $f_{\text{ext}}(x,t)=-d/dxV_{\text{ext}}(x-ct)$, and the properties of the system can be studied by considering the equation governing $p(x,v,t)$, the density distribution in phase space of a single particle. The associated Kramers equation[25,26] reads as

$$\frac{\partial}{\partial t}p(x,v,t)+\left[v\frac{\partial}{\partial x}+\frac{f_{\text{ext}}(x-ct)}{m}\frac{\partial}{\partial v}\right]p(x,v,t)=\gamma\left[\frac{\partial}{\partial v}v+\frac{T_o}{m}\frac{\partial^2}{\partial v^2}\right]p(x,v,t). \tag{3}$$

We assume that the shifting external potential is localized within a finite region and vanishes outside. Therefore, far away from such a region, we should have a time independent equilibrium distribution $p_o(x,v)=\rho_o\exp(-v^2/(2v_T^2))/(\sqrt{2\pi}v_T)$, where ρ_o is the density of particles and $v_T=\sqrt{k_BT_o/m}$ is the Gaussian width for their velocity distribution. For a static external potential, i.e., the $c=0$ limit of Eq. (1), the distribution $p(x,v,t)$ would evolve in time toward the thermal equilibrium value $p_{\text{eq}}(x,v)=p_o(x,v)\exp(-V_{\text{ex}}(x)/k_BT_o)$, which would be reached (sooner or later) from any initial distribution $p(x,v,0)$. For $c\neq 0$, the continuous shift of the external potential implies a permanent perturbation of the thermal equilibrium, but still there would be a transient evolution from any $p(x,v,0)$ to a unique stationary state $\tilde{p}(x-ct,v)$ in which the time dependence is reduced to a shift of the x coordinate, to follow the external potential $V_{\text{ext}}(x-ct)$. This steady state is the object of the present study. All of the results presented here may be translated to a purely static distribution in the presence of a time independent external potential $V(x)=-f_ox+V_{\text{ext}}(x)$, with a constant slope plus the same potential barrier which we considered in Eq. (3). The time derivative in the first term of Eq. (3) vanishes, but there is an extra term proportional to f_o to take into account the constant background force added to the localized barrier force $f_{\text{ext}}(x)$. Away from the barrier, the particles move at constant mean velocity $v_o=f_o/(m\gamma)$, and a change of reference framework from v to $v'\equiv v-v_o$ leads to exactly the same equation [Eq. (3)] for $p(x,v',t)$, when the barrier appears as moving at rate $c=-v_o$. These two equivalent versions of the same problem have been studied within the DDFT formalism,[12,27–29] valid for large γ. The same exact mapping between the moving barrier in a flat background and the static barrier in a sloped potential would be valid for partially damped systems explored here.

It is convenient to introduce the following dimensionless variables:

$$\tau\equiv tv_T\rho_o,\quad V\equiv\frac{v}{v_T},\quad X\equiv x\rho_o,\quad C\equiv\frac{c}{v_T}, \tag{4}$$

$$\Gamma\equiv\frac{\gamma}{v_T\rho_o},\quad F_{\text{ext}}(X,\tau)\equiv\frac{f_{\text{ext}}(x-ct)}{mv_T^2\rho_o},\quad P(X,V,\tau)\equiv\frac{v_T}{\rho_o}p(x,v,t). \tag{5}$$

Accordingly, Kramers' evolution equation for the phase space distribution function can be rewritten with the help of relations (4) and (5) as

$$\frac{1}{\Gamma}\frac{\partial P(X,V,\tau)}{\partial \tau} = L_{\rm FP}P(X,V,\tau) - \frac{1}{\Gamma}V\frac{\partial}{\partial X}P(X,V,\tau) - \frac{1}{\Gamma}F_e(X,\tau)\frac{\partial}{\partial V}P(X,V,\tau) \tag{6}$$

having introduced the "Fokker–Planck" operator $L_{\rm FP}$, whose eigenfunctions $H_\mu(V)$ have the following property:

$$L_{\rm FP}H_\mu(V) \equiv \frac{\partial}{\partial V}\left[\frac{\partial}{\partial V} + V\right]H_\mu(V) = -\mu H_\mu(V), \tag{7}$$

for $\mu=0,1,\ldots$, and have the explicit representation,

$$H_\mu(V) \equiv \frac{1}{\sqrt{2\pi}}(-1)^\mu\frac{\partial^\mu}{\partial V^\mu}\exp\left(-\frac{1}{2}V^2\right). \tag{8}$$

It is convenient to define raising and lowering operators in the eigenfunctions series, $a_\pm H_\mu(V)=H_{\mu\pm1}(V)$, so that the contributions of the damping and the external forces in the last two terms of Eq. (6) may be represented through

$$VH_\mu(V) = H_{\mu+1} + \mu H_{\mu-1}(V) \equiv (a_+ + \mu a_-)H_\mu(V) \tag{9}$$

and

$$\frac{\partial H_\mu}{\partial V} = -H_{\mu+1}(V) \equiv -a_+H_\mu(V). \tag{10}$$

The exact solutions of Eq. (6) in the regions where the external force vanishes may be written in terms of the infinite series of modes, $\mu=0,1,\ldots$, with the generic form[17]

$$P^{(\mu)}(X,V,\tau) = \exp(-\mu\Gamma\tau)\exp\left[-\frac{a_+}{\Gamma}\frac{\partial}{\partial X}\right] \times\left(1+\frac{a_-}{\Gamma}\frac{\partial}{\partial X}\right)^\mu H_\mu(V)\phi^{(\mu)}(X,\tau). \tag{11}$$

The function $\phi^{(\mu)}(X,\tau)$, which fully defines the mode $\tilde{P}^{(\mu)}(X,V,\tau)$, represents any solution of the diffusion equation

$$\frac{\partial}{\partial\tau}\phi^{(\mu)}(X,\tau) = \frac{1}{\Gamma}\frac{\partial^2}{\partial X^2}\phi^{(\mu)}(X,\tau). \tag{12}$$

From Eq. (11) in the case $\mu=0$, we explicitly obtain

$$P^{(0)}(X,V,\tau) = H_0(V)\phi^{(0)}(X,\tau) - \frac{H_1(V)}{\Gamma}\frac{\partial\phi^{(0)}(X,\tau)}{\partial X} + \frac{H_2(V)}{2!\Gamma^2}\frac{\partial^2\phi^{(0)}(X,\tau)}{\partial X^2} + \cdots, \tag{13}$$

which describes a density inhomogeneity, represented by the term $\phi^0(X,\tau)$, and the associated momentum current, the term of the order of $1/\Gamma$, kinetic energy current, the term of the order of $1/\Gamma^2$, and so on. These terms are *slaved* by the density and their shapes are given by the successive derivatives of $\phi^0(X,\tau)$ with respect to X. Similarly, from Eq. (11), the solution with $\mu=1$ has the explicit representation

$$P^{(1)}(X,V,\tau) = \exp(-\Gamma\tau)\left[\left(H_1(V)\phi^{(1)}(X,\tau) - \frac{H_2(V)}{\Gamma}\frac{\partial\phi^{(1)}(X,\tau)}{\partial X} + \frac{H_3(V)}{2!\Gamma^2}\frac{\partial^2\phi^{(1)}(X,\tau)}{\partial X^2} + \cdots\right) + \frac{1}{\Gamma}\left(H_0(V)\frac{\partial\phi^{(1)}(X,\tau)}{\partial X} - \frac{H_1(V)}{\Gamma}\frac{\partial^2\phi^{(1)}(X,\tau)}{\partial X^2} + \cdots\right)\right], \tag{14}$$

where the first line in the right hand side has the interpretation of a *master* current inhomogeneity $\phi^{(1)}(X,\tau)$, which slaves higher order moments with decreasing amplitudes $(1/\Gamma,\ldots)$, while the second line in the right hand side has the same structure as $P^{(0)}(X,V,\tau)$ with amplitude $\phi^{(0)}=\Gamma^{-1}\partial_X\phi^{(1)}$, and both terms have fast decay of the exponential prefactor. The physical interpretation of such a combination is that an initially pure current fluctuation, which is described by $H_1(V)\phi_1(X,0)$, would die very fast, as $\exp(-\Gamma\tau)$, but leaving a density fluctuation proportional to $\Gamma^{-1}\partial_X\phi^{(1)}\times(X,0)$ behind, which would evolve diffusively. The particular combination in Eq. (14) is such that it completely cancels the remnant density fluctuations, i.e., it orthogonalizes $P^{(1)}(X,V,\tau)$ to $P^{(0)}(X,V,\tau)$, and leaves a purely *fast* decaying form. The generic free mode of the order of μ, is a master term $\phi^{(\mu)}(X,\tau)H_\mu(V)\exp(-\Gamma\tau)$, representing a density $(\mu=0)$, current $(\mu=1)$, temperature $(\mu=2)$, heat $(\mu=3)$, etc., perturbation of the equilibrium distribution $p_o(x,v)$. The master distribution $\phi^{(\mu)})(X,\tau)$ slaves the perturbation components associated with any other $H_{\mu'}(V)$, with increasing powers of the inverse damping $1/\Gamma$, so that the whole distribution $P^{(\mu)}(X,V,\tau)$ decays toward equilibrium with an exponential decay time $(\mu\Gamma)^{-1}$. For time independent external potentials, the high order modes are only visible as very short transient states of $P(X,V,\tau)$ toward $p_o(x,v)$, and in the large damping limit, $\Gamma\gg1$, the modes are essentially reduced to their master component.[17] In this work, we analyze the role of these modes under the continuous shift of the external potential, for finite values of the damping constant Γ.

III. STEADY STATE SOLUTION

A. The steady state form of the free modes

Now, we impose the steady state condition $P(X,V,\tau)=\tilde{P}(X-C\tau,V)$, which shifts with time to follow the boundary conditions in the moving potential barrier, in terms of the variable $\tilde{X}=X-C\tau$. We analyze first the form of the free modes of the expansion to represent the solution of Eq. (6) in the regions where the external force vanishes. Since the steady solution has the property

$$\frac{\partial}{\partial\tau}[P^{(\mu)}(X,V,\tau)] = -C\frac{\partial}{\partial X}[P^{(\mu)}(X,V,\tau)], \tag{15}$$

it follows that

$$\frac{\partial}{\partial\tau}[\exp(-\mu\Gamma\tau)\phi^{(\mu)}(X,\tau)] = -C\exp(-\mu\Gamma\tau)\frac{\partial}{\partial X}[\phi^{(\mu)}(X,\tau)], \quad (16)$$

so that we can transform the diffusion equation [Eq. (12)] for the master distribution into an ordinary differential equation

$$\frac{\partial^2}{\partial X^2}\phi^{(\mu)}(X,\tau) + \Gamma C\frac{\partial}{\partial X}\phi^{(\mu)}(X,\tau) - \mu\Gamma^2\phi^{(\mu)}(X,\tau) = 0, \quad (17)$$

whose solutions are proportional to $\exp(\beta_\pm^{(\mu)}X)$ with

$$\frac{\beta_\pm^{(\mu)}}{\Gamma} = \frac{-C \pm \sqrt{C^2+4\mu}}{2}. \quad (18)$$

Finally, the product $\exp(-\mu\Gamma\tau)\phi^{(\mu)}(X,\tau)$ featured in Eq. (11) has the form consistent with Eq. (15):

$$\exp(-\mu\Gamma\tau)\phi^{(\mu)}(X,\tau) = \sum_{\zeta=\pm} A_\zeta^{(\mu)}\exp[\beta_\zeta^{(\mu)}(X-C\tau)]. \quad (19)$$

The amplitudes $A_\pm^{(\mu)}$ determine the contribution of each mode in any region where the external potential vanishes. Since we assumed that the potential barrier is restricted to a finite region around $\tilde{X}\equiv X-C\tau\approx 0$, we shall refer the positive values of $\tilde{X}$ as the front region, whereas the negative values of $\tilde{X}$ represent the wake region.

For the first mode, $\mu=0$, the exponent $\beta_+^{(0)}$ vanishes, so that $A_+^{(0)}=1$, to represent the only possible constant contribution to $P(X,V,\tau)$, the equilibrium distribution $p(x,v,t)=\rho_o H_o(v/v_T)/v_T$, away from the perturbation. The second exponent for $\mu=0$, is $\beta_-^{(0)}=-\Gamma C$, so that it can only contribute to $P(X-C\tau,V)$ in the *front* region of the advancing potential barrier, with an amplitude $A_-^{(0)}$ to be fixed by the boundary condition at the advancing front of the external barrier. In the left region behind the barrier, the amplitude $A_-^{(0)}$ has to vanish, since otherwise $P^{(0)}(X-C\tau,V)$ would diverge as $\exp(-CX)$ for $X\ll 0$. Therefore, substituting the solution (19) with $\mu=0$ into Eq. (13), we obtain the structure

$$\tilde{P}^{(0)}(\tilde{X},V) = H_0(V) + A_-^{(0)}e^{-\Gamma C\tilde{X}}\left[H_0(V) + CH_1(V) + \frac{C^2H_2(V)}{2!} + \cdots\right], \quad (20)$$

for $\tilde{X}=X-C\tau$ in the front side of the advancing barrier, while behind the barrier, we have the pure equilibrium structure $\tilde{P}^{(0)}(\tilde{X},V)=H_0(V)$, with no remnant *wake* structure.

The contribution proportional to $H_0(V)$ in $P^{(0)}(\tilde{X},V)$ has precisely the shape obtained from the analysis of Eq. (1) in the strong damping limit,[12] when the particles are always at their velocity limit and the inertial term can be neglected. In this limit, the Smoluchowski[30] description of the system is sufficient, and the solution can be written as $P(X,V,\tau)=\rho(X,\tau)H_o(V)/\rho_o$, where $\rho(X,\tau)$ satisfies the following diffusion equation with drift:

$$\frac{\partial\rho(X,\tau)}{\partial\tau} = \frac{1}{\Gamma}\frac{\partial^2\rho(X,\tau)}{\partial X^2} - \frac{1}{\Gamma}\frac{\partial}{\partial X}(\rho(X,\tau)F_e(X-C\tau)), \quad (21)$$

and the stationary solution $\rho(X-C\tau)$ for shifting potential barriers has the exponential front and the complete lack of wake identical to the $H_0(V)$ contribution to Eq. (20). The only qualitative difference between the fully damped system described by the Smoluchowski equation, and the $\mu=0$ mode solution of Eq. (20) is that the front density perturbation slaves a current $CH_1(V)$, a kinetic energy increase $C^2H_2(V)/2$, and similar higher order terms which may be resumed to give exactly the form

$$\tilde{P}^{(0)}(\tilde{X},V) = H_0(V) + A_-^{(0)}e^{-\Gamma C\tilde{X}}H_0(V-C), \quad (22)$$

i.e., the whole perturbation of $\tilde{P}^{(0)}(\tilde{X},V)$ over the equilibrium value $H_0(V)$ has a Maxwellian distribution of velocities but shifted to the reference frame of the advancing potential barrier.

All higher order terms are characterized by $\beta_+^{(\mu)}>0$ and $\beta_-^{(\mu)}<0$, so that the exponent $\beta_-^{(\mu)}$, has to be taken at the front side and $\beta_+^{(\mu)}$ behind the barrier, so that there is one free amplitude $A_\pm^{(\mu)}$ for each mode at each side of the barrier. The distribution functions for these modes may also be written in terms of the shifted eigenfunctions of the operator $L_{\rm FP}$, $H_\nu(V+\beta_\pm^{(\mu)}/\Gamma)$. Thus, the $\mu=1$ mode has the form

$$\tilde{P}^{(1)}(\tilde{X},V) = A_\pm^{(1)}e^{\beta_\pm^{(1)}\tilde{X}}\left[H_1\left(V+\frac{\beta_\pm^{(1)}}{\Gamma}\right) + \frac{\beta_\pm^{(1)}}{\Gamma}H_0\left(V+\frac{\beta_\pm^{(1)}}{\Gamma}\right)\right], \quad (23)$$

whereas for the $\mu=2$ mode, we find

$$\tilde{P}^{(2)}(\tilde{X},V) = A_\pm^{(2)}e^{\beta_\pm^{(2)}\tilde{X}}\left[H_2\left(V+\frac{\beta_\pm^{(2)}}{\Gamma}\right) + 2\frac{\beta_\pm^{(2)}}{\Gamma}H_1\left(V+\frac{\beta_\pm^{(2)}}{\Gamma}\right) + \left(\frac{\beta_\pm^{(2)}}{\Gamma}\right)^2 H_0\left(V+\frac{\beta_\pm^{(2)}}{\Gamma}\right)\right], \quad (24)$$

and the generic structure of the μ mode is

$$\tilde{P}^{(\mu)}(\tilde{X},V) = A_\pm^{(\mu)}e^{\beta_\pm^{(\mu)}\tilde{X}}\left(1+\frac{\beta_\pm^{(\mu)}a_-}{\Gamma}\right)^\mu H_\mu\left(V+\frac{\beta_\pm^{(\mu)}}{\Gamma}\right). \quad (25)$$

Notice that all $P^{(\mu)}(\tilde{X},V)$ contributions for $\mu>0$ exponentially decay away from the barrier.

The inclusion of higher order terms creates a wake density fluctuation structure, with exponential decays $\exp(\beta_+^{(\mu)}\tilde{X})$, which have $\beta_+^{(\mu)}\approx\sqrt{\mu}$ for $C\ll 1$ and $\beta_+^{(\mu)}\sim\mu/C\ll\mu$ for $C\gg\mu$. The front density structure contains several exponential decays $\exp(\beta_-^{(\mu)}\tilde{X})$, with $\beta_-/\Gamma\approx-\sqrt{\mu}$ for $C\ll 1$ and $\beta_+^{(\mu)}/\Gamma\approx -C$ for $C\gg\mu$. Both at the front and the wake regions, the density fluctuations go together with fluctuations in the velocity distribution, which may be described as shifted equilibrium distributions, $H_0(V+\beta_\pm^{(\nu)})$, shifted current distributions $H_1(V+\beta_\pm^{(\nu)})$, etc. The front region is broad if the damping is weak and the barrier velocity small because the restoring force is proportional to the velocity of the

colloidal particles with respect to the quiescent solvent. The velocity distribution changes in front of the barrier and develops secondary peaks at $V=C$, $V=-\beta_-^{(1)}/\Gamma$, $V=-\beta_-^{(2)}/\Gamma$, etc.

B. Generic properties of the steady state produced by a shifting barrier

We now consider the generic solution of Eq. (6), including the regions inside the moving barrier, where we have to include the force term. The steady state condition $P(X,V,\tau)=P(X-C\tau,V)\equiv\tilde{P}(\tilde{X},V)$ transforms Eq. (6) into

$$(V-C)\frac{\partial\tilde{P}(\tilde{X},V)}{\partial\tilde{X}}=\Gamma L_{\mathrm{FP}}\tilde{P}(\tilde{X},V)-F_e(\tilde{X})\frac{\partial\tilde{P}(\tilde{X},V)}{\partial V}. \tag{26}$$

The general solution of this equation may be represented as

$$\tilde{P}(\tilde{X},V)=\sum_{\nu=0}^{\infty}\Phi_\nu(\tilde{X})H_\nu(V), \tag{27}$$

with generic functions $\Phi_\nu(\tilde{X})$, to be determined from the projections of Eq. (26) on each of the FP eigenfunctions $H_\nu(V)$. The projections for $\nu=0$ and $\nu=1$ give

$$\frac{\partial\Phi_1(\tilde{X})}{\partial\tilde{X}}-C\frac{\partial\Phi_0(\tilde{X})}{\partial\tilde{X}}=0 \tag{28}$$

and

$$2\frac{\partial\Phi_2(\tilde{X})}{\partial\tilde{X}}-C\frac{\partial\Phi_1(\tilde{X})}{\partial\tilde{X}}+\frac{\partial\Phi_0(\tilde{X})}{\partial\tilde{X}}=F_e(\tilde{X})\Phi_0(\tilde{X})-\Gamma\Phi_1(\tilde{X}). \tag{29}$$

The general form for any $\nu\geqslant 1$ is

$$(\nu+1)\frac{\partial\Phi_{\nu+1}(\tilde{X})}{\partial\tilde{X}}-C\frac{\partial\Phi_\nu(\tilde{X})}{\partial\tilde{X}}+\frac{\partial\Phi_{\nu-1}(\tilde{X})}{\partial\tilde{X}}$$
$$=F_e(\tilde{X})\Phi_{\nu-1}(\tilde{X})-\nu\Gamma\Phi_\nu(\tilde{X}). \tag{30}$$

In the absence of the force term $F_e(X)$, the general solution of this (infinite) set of coupled ordinary linear differential equations may be written in terms of the free modes [Eq. (25)], with arbitrary amplitudes $A_+^{(\mu)}$ at the back side, and $A_-^{(\mu)}$ at the front side of the moving barrier.

The structure of Eq. (28) is independent of $F_e(\tilde{X})$, and it represents the continuity equation, relating the mass density $\rho(\tilde{X})\equiv\rho_o\Phi_0(\tilde{X})$ to the current density $j(\tilde{X})\equiv\rho_o\Phi_1(\tilde{X})$, to keep the mass balance under a steady flow,

$$\frac{\partial j(X,\tau)}{\partial X}=C\frac{\partial\rho(X-C\tau)}{\partial X}. \tag{31}$$

The integration of Eq. (28) from the boundary conditions $\Phi_0(\tilde{X})=1$ and $\Phi_1(\tilde{X})=0$, far away from the moving barrier, gives

$$\Phi_1(\tilde{X})=C(\Phi_0(\tilde{X})-1), \tag{32}$$

i.e., any positive excess $\Phi_0(\tilde{X})-1\geqslant 0$ in the distribution of particles near the moving barrier is associated with a current $j(\tilde{X})=C(\rho(\tilde{X})-\rho_o)$ following the barrier shift. The regions with $\Phi_0(\tilde{X})\leqslant 1$ imply a depletion of the density and a countercurrent with opposite sign to the barrier displacement. In the strong damping limit[12] such a depletion and countercurrent were limited to the interior of the potential barrier, since there was no wake left behind it. Here, the inertial effects included open the possibility of such wake, so that we may find regions outside of the moving barrier where the mean velocity $\langle V\rangle=\Phi_1(\tilde{X})/\Phi_0(\tilde{X})=C[1-1/\Phi_0(\tilde{X})]$ has sign opposite to C.

Equation (29), from the projection of Eq. (26) on $H_1(V)$, represents the local balance of momentum. If we integrate it across the whole inhomogeneity, from far, from the rear to far, from the front of the moving potential barrier, the integrals of all the derivatives vanish, and we obtain that the total force F_T, produced by the barrier on the particles balances the friction force created by the bath on the total current

$$F_T\equiv\int_{-\infty}^{\infty}d\tilde{X}F_e(\tilde{X})\Phi_0(\tilde{X})=\Gamma\int_{-\infty}^{\infty}d\tilde{X}\Phi_1(\tilde{X}), \tag{33}$$

i.e., it gives the global force balance in the system. Notice that only the region of potential barrier contributes to the first integral in the left hand side, while the entire volume contributes to the right hand side.

The integration of Eq. (29) from $\Phi_0(X)=1$, $\Phi_1(X)=0$, and $\Phi_2(X)=0$, at any point far from the barrier gives the local excess of kinetic energy at any point,

$$\Phi_2(\tilde{X})=\frac{1}{2}\left[C\Phi_1(\tilde{X})-\Phi_0(\tilde{X})-1+\int_{-\infty}^{\tilde{X}}d\tilde{X}(F_e(\tilde{X})\Phi_0(\tilde{X})\right.$$
$$\left.-\Gamma\Phi_1(\tilde{X}))\right]. \tag{34}$$

Therefore, once we have the particle distribution $\Phi_0(\tilde{X})$, we may obtain the mean velocity of the particles $\langle V\rangle=\Phi_1(\tilde{X})/\Phi_0(\tilde{X})$ from Eq. (32), and their local temperature relative to that of the bath, $T(\tilde{X})/T_o=1+\Phi_2(\tilde{X})/\Phi_0(\tilde{X})$ from Eq. (34).

Similarly, the equation for $\nu=2$ in the series [Eq. (30)] corresponds to the energy balance. Its integration from a point far behind the barrier to an arbitrary point $\tilde{X}$ gives direct access to the heat current $\Phi_3(\tilde{X})$, while its integral across the whole inhomogeneity gives the total power transferred from the barrier to the particles

$$\mathcal{W}\equiv\int_{-\infty}^{\infty}d\tilde{X}F_e(\tilde{X})\Phi_1(\tilde{X})=2\Gamma\int_{-\infty}^{\infty}d\tilde{X}\Phi_2(\tilde{X}), \tag{35}$$

where the last integral has to be interpreted as the total heat dissipated by the particles due to the local temperature difference over the bath, $\Phi_2=\Phi_0(\tilde{X})(T(\tilde{X})/T_o-1)$. Notice that the steady state conditions, and the fact that the potential

energy vanishes both at the front and at the rear of the moving barrier, gives a direct relation, $\mathcal{W}=CF_T$, between the power and the force. Through Eqs. (32), (33), and (35) we also obtain a relationship between the total excess of particles and the excess kinetic energy. Written in terms of the original variables,

$$\int dx\rho(x)(T(x)-T_o)=\frac{mc^2}{2}\int dx(\rho(x)-\rho_o), \tag{36}$$

this should be a generic property of the steady state distributions, independent of the damping Γ.

C. Expansion in terms of the steady free modes

The above expressions for $\Phi_1(\tilde{X}),\Phi_2(\tilde{X}),\ldots$, given in terms of $\Phi_0(\tilde{X})$ can only be used after the whole set of ordinary differential Eqs. (28)–(30) are solved. That requires either a resumation of all the terms, as done for the free modes in Eq. (22), or some truncation scheme to perform a numerical integration for the regions with $F_e(\tilde{X})\neq 0$. Unless the force is very weak everywhere, a direct truncation scheme of the expansion in Eq. (27), e.g., taking $\Phi_3(\tilde{X})=0$, and solving the first three equations to get $\Phi_0(\tilde{X})$, $\Phi_1(\tilde{X})$, and $\Phi_2(\tilde{X})$, leads to unphysical results, strongly dependent on the order of the truncation. On the contrary, we have found very good convergence, at least for any $\Gamma\geqslant 1$, using a finite parametrization of $\tilde{P}(\tilde{X},V)$ based on the natural modes for the free particles. We fix the number $\mu_{\max}$ of such modes to be used in the front and in the wake regions, so that the solution, $\tilde{P}(\tilde{X},V)$, is described by $\mu_{\max}+1$ constants $A_-^{(\mu)}$ at the first region, and $\mu_{\max}$ constants $A_+^{(\mu)}$ at the second region, besides the trivial contribution $A_+^{(0)}=1$. Within the barrier region we use $2\mu_{\max}+1$ independent functions, $\psi_\pm^{(\mu)}(\tilde{X})$ to parametrize $P(\tilde{X},V)$ as

$$\tilde{P}(\tilde{X},V)=\sum_{\mu=0}^{\mu_{\max}}\sum_{\zeta=\pm}\psi_\zeta^{(\mu)}(\tilde{X})\left(1+\frac{\beta_\zeta^{(\mu)}a_-}{\Gamma}\right)^{\mu}H_\mu\left(V+\frac{\beta_\zeta^{(\mu)}}{\Gamma}\right). \tag{37}$$

Therefore, each term Φ_ν in the expansion [Eq. (27)] is expressed as a linear combination of the functions $\psi_\pm^{(\mu)}(\tilde{X})$ to be determined by means of Eqs. (28)–(30), for all values $\nu\leqslant 2\mu_{\max}+1$.

The simplest parametrization within this scheme corresponds to include only the $\mu=0$ mode, with $\beta_+^{(0)}=0$ and $\beta_-^{(0)}=-C\Gamma$, so that

$$P(\tilde{X},V)=\psi_+^{(0)}(\tilde{X})H_0(V)+\psi_-^{(0)}(\tilde{X})H_0(V-C). \tag{38}$$

Hence, all the terms in expansion [Eq. (27)] are given in terms of these two functions,

$$\Phi_0(\tilde{X})=\psi_+^{(0)}(\tilde{X})+\psi_-^{(0)}(\tilde{X}),\quad \Phi_1(\tilde{X})=C\psi_-^{(0)}(\tilde{X}),$$
$$\Phi_2(\tilde{X})=\frac{C^2}{2!}\psi_-^{(0)}(\tilde{X})\quad \text{etc.} \tag{39}$$

The projections of Eq. (26) on the first two FP eigenfunctions are enough to determine $\psi_+^{(0)}(\tilde{X})$ and $\psi_-^{(0)}(\tilde{X})$. From Eq. (28), we obtain that $\psi_+^{(0)}(\tilde{X})$ has to be constant all over the system, both inside and outside the potential barrier, therefore, it is fixed by the asymptotic value $\psi_+^{(0)}(\tilde{X})=1$, and we may use the particle distribution $\Phi_0(\tilde{X})=1+\psi_-^{(0)}(\tilde{X})$ as the only free functional variable. Regarding now the projection on $H_1(V)$, we obtain that the contributions from the derivatives of $\Phi_1(\tilde{X})$ and $\Phi_2(\tilde{X})$ on the left hand side of Eq. (29) cancel each other, so that

$$\frac{\partial\Phi_0(\tilde{X})}{\partial\tilde{X}}=F_e(\tilde{X})\Phi_0(\tilde{X})-C\Gamma(\Phi_0(\tilde{X})-1). \tag{40}$$

which is exactly the DDF equation obtained and solved by Penna and Tarazona[12] from the integration of Eq. (21). Notice that this simplest parametric description of $P(\tilde{X},V)$ is, therefore, consistent with respect to the mass and momentum balances, but it has no flexibility to recover the equivalent balances of energy ($\nu=2$), heat current ($\nu=3$), etc., required by Eq. (30). A direct substitution of Eq. (39) into Eq. (30) shows that the local balance for $\nu\geqslant 2$ fails by a term $C^{\nu-1}F_e(\tilde{X})/(\nu-1)!$, at each $\nu\geqslant 2$. Such a failure is less important for low shifting rate, $C\ll 1$, and for modes $\nu\gg C$. Also, the global balance represented by Eqs. (33)–(35) would be kept at any order ν, since the total integral of $F_e(\tilde{X})$ has to vanish. The inertial effects appear to recover the local balances missed by the DDF approximation, and we may include them in a systematic way including in $\tilde{P}(\tilde{X},V)$ the contributions of the higher order free modes. That enlarges the set of free functions $\psi_\pm^{(\mu)}(\tilde{X})$, and allow the solution of Eq. (26) up to higher order eigenfunctions of the FP operator.

IV. NUMERICAL RESULTS FOR A PARABOLIC POTENTIAL BARRIER

As an application we study a parabolic potential barrier of the form, $U(\tilde{X})=\kappa(1-\tilde{X}^2)/2$ creating a linear force $F_e(\tilde{X})=\kappa\tilde{X}$, restricted to the interval $-1\leqslant\tilde{X}\leqslant 1$. As we consider only the steady case we have to solve Eq. (30) within the barrier, and to find the solutions matching with the physical solutions Eq. (25) at the front ($\tilde{X}\geqslant 1$) and at the wake ($\tilde{X}\leqslant -1$). The matching of $\tilde{P}(\tilde{X},V)$ inside and outside the barrier is achieved by requiring that $\tilde{P}(\tilde{X},V)$ in Eq. (26) should be continuous at $\tilde{X}=\pm 1$, but with a discontinuous first derivative with respect to $\tilde{X}$, to match the discontinuity in $F_e(\tilde{X})$, i.e.,

$$(V-C)\left(\left.\frac{\partial\tilde{P}(\tilde{X},V)}{\partial\tilde{X}}\right|_{\tilde{X}=1+\epsilon}-\left.\frac{\partial\tilde{P}(\tilde{X},V)}{\partial\tilde{X}}\right|_{\tilde{X}=1-\epsilon}\right)=\kappa\left.\frac{\partial\tilde{P}(\tilde{X},V)}{\partial V}\right|_{\tilde{X}=1}, \tag{41}$$

and a similar condition at $\tilde{X}=-1$. Most of the results presented here have been obtained with $\mu_{\max}=4$, i.e., with nine

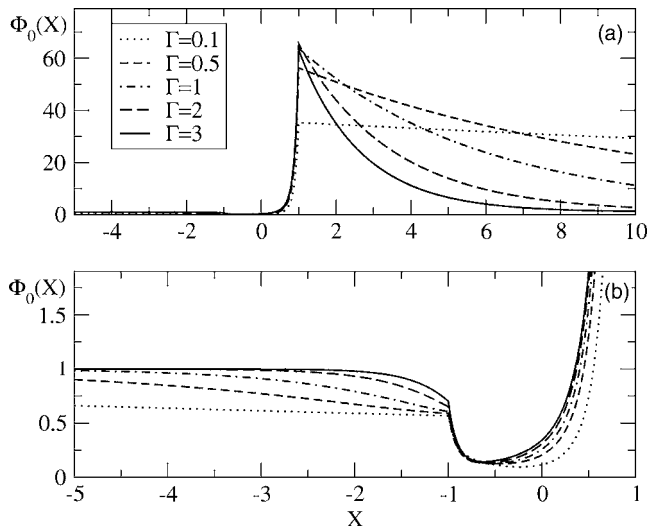

FIG. 1. Steady state scaled density profile, $\Phi_0(X)=\rho(X)/\rho_o$, in the reference frame of the moving parabolic barrier. The barrier strength is $\kappa=10$, its width is 2 and moves at a relatively low velocity, $C=0.2$, while the damping constant Γ takes on several values. Panel (b) shows the structure of the region within the barrier $(-1\leqslant X\leqslant 1)$, and the inertial wake left behind by the advancing barrier. The position X is relative to the barrier. Adimensional units [Eqs. (4) and (5)] are used for all the quantities.

independent functions $\psi_{\pm}^{(\mu)}(\tilde{X})$, besides the trivial $\psi_{+}^{(0)}=1$, to ensure the correct projection of Eq. (26) up to the order of $H_9(V)$. Nearly identical results are obtained with $\mu_{\max}=3$, and even with $\mu_{\max}=2$ for $\Gamma\geqslant 2$. However, qualitative differences appear with respect to the DDF result ($\mu_{\max}=0$), unless we have both large damping Γ and a low shifting rate C for the barrier. In any case, we have to deal with a set of linear differential equations, with a shooting boundary problem, to get the physical match with the free modes, so that $A_{+}^{(\mu)}=0$ at $\tilde{X}=1$, and $A_{-}^{(\mu)}=0$ at $\tilde{X}=-1$.

In Fig. 1, we present results for a high potential barrier, $\kappa=10$, moving with respect to the bath at a relatively low velocity, $C=0.2$. For large damping, the system is in the strong drift limit.[12] The density distribution is strongly depleted within the barrier, while the density in the front region grows to a large value, more than 60 times the asymptotic density in this case, so that there are enough particles going over the barrier to keep the stationary state. We observe that for $\Gamma\geqslant 1$, the inertial effects have little influence in the structure of the front region. When $\Phi_0(\tilde{X})$ is rescaled in terms of $\Gamma(\tilde{X}-1)$, as in Fig. 2(a), the curves collapse into a single large Γ limit. This is consistent with the fact that the velocity distribution at the front region is dominated by the shifted Maxwellian form [Eq. (38)]. The effect of reducing Γ below a value of 1 renders smaller the amplitude of the exponential contribution in the formula $\Phi_0(X)=1+A\exp(-C\Gamma X)$. Nevertheless, for the lowest value of Γ presented in that figure the expansion in modes is still far from convergence for $\mu_{\max}=4$.

In Fig. 2(b), we present the structure of the wake by rescaling the distance from the left edge of the barrier by the ΓC factor. The profile saturates for low Γ, while is continuously reduced as Γ increases. This is consistent with the no-wake prediction in the large damping limit, when the inertial effects are fully suppressed. Nevertheless, the decrease in the wake structure with increasing Γ is very slow, so that the presence of such region, with $\rho(x)<\rho_o$ and, hence, mean velocity $\langle v\rangle=v_T(1-\rho_o/\rho(x))<0$, behind the shifting potential barrier, is an important qualitative effect induced by the inertial dynamics of the particles, and which was neglected within the DDF analysis.[12]

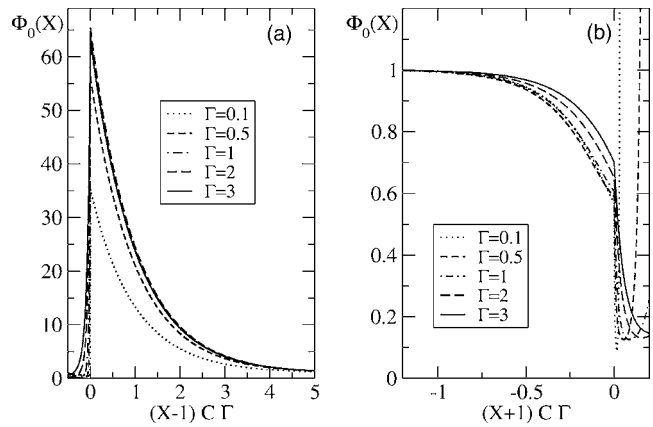

FIG. 2. Scaled density profile, $\Phi_0(X)=\rho(X)/\rho_o$, at the front (a) and wake (b) regions in Fig. 1 is presented in reduced distances $(X\pm 1)C\Gamma$, to take into account the natural decay length of the zeroth order mode. The front structure curves collapse for $\Gamma\geqslant 1$, while the wake region is reduced for increasing Γ. The position X is relative to the barrier. Adimensional units [Eqs. (4) and (5)] are used for all the quantities.

In Fig. 3, we present the results for the same barrier, as in Fig. 1, but with a much larger velocity $C=2$. In the large damping limit such a situation corresponds to a "high countercurrent" regime,[12] in which the barrier moves too fast to produce a strong perturbation in the density distribution. When the bath damping parameter is reduced, the inertial dynamics creates a strong amplification of the front structure, which is now much more symmetric with respect to the ad-

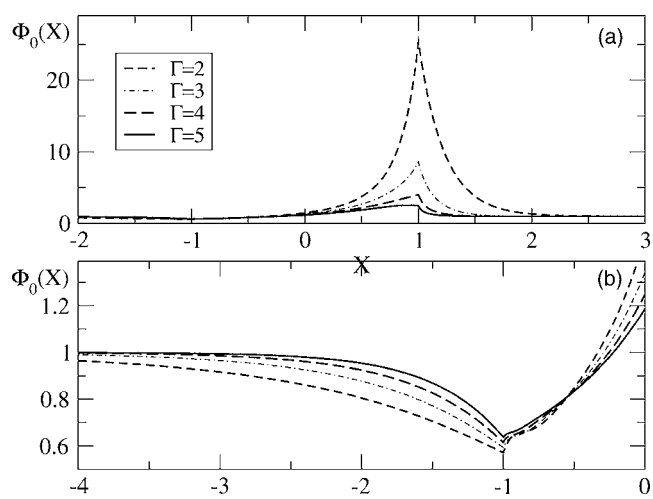

FIG. 3. Steady state density distribution, $\Phi_0(X)=\rho(X)/\rho_o$, induced by the same potential barrier as in Fig. 7, but moving at a higher velocity, $C=2$. The damping constants are $\Gamma=5$ (full line), $\Gamma=4$ (long-dashed line), $\Gamma=3$ (dot-dashed line), and $\Gamma=2$ (short-dashed line). Panel (a) gives a general view of the high density structure at the advancing front. Panel (b) shows the structure of the depleted region within the barrier $(-1\leqslant X\leqslant 1)$, and the inertial wake left behind by the advancing barrier. The position X is relative to the barrier. Adimensional units [Eqs. (4) and (5)] are used for all the quantities.

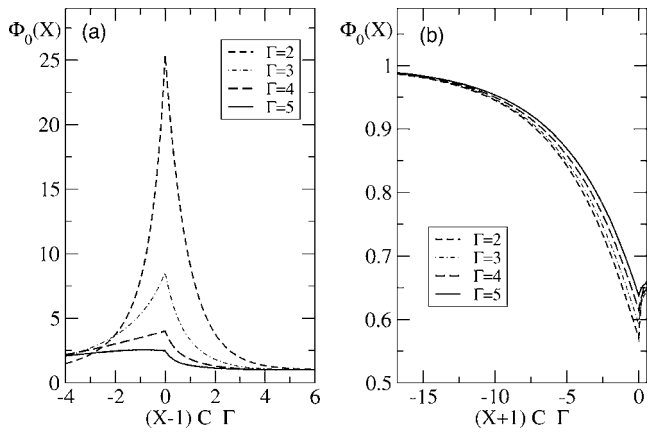

FIG. 4. The structure of the relative density $\Phi_0(X)=\rho(X)/\rho_o$, at the front (a) and wake (b) regions in Fig. 3 is presented in reduced distances $(X\pm 1)C\Gamma$, to take into account the natural decay length of the zeroth order mode. The position X is relative to the barrier. Adimensional units [Eqs. (4) and (5)] are used for all the quantities.

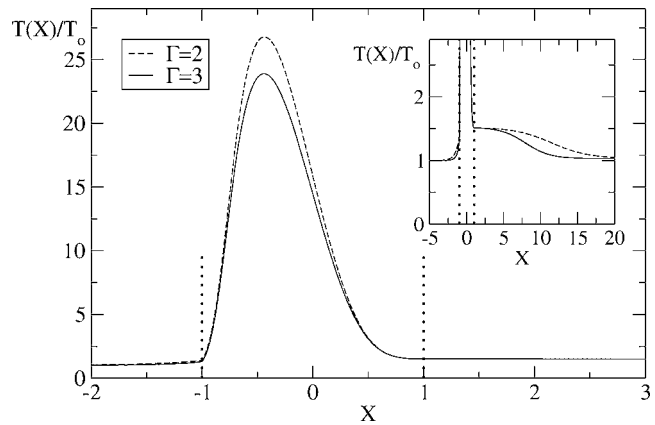

FIG. 5. Steady state temperature profile induced by a parabolic potential barrier shifted at rate $C=0.2$. The position X is relative to the barrier and the vertical dotted lines are the barrier edges. The inset shows the structure of for $T(X)\approx T_o$. Adimensional units [Eqs. (4) and (5)] are used for all the quantities.

vancing barrier front at $\tilde{X}=1$. Roughly speaking, half of the particles at the front region are actually within the potential barrier, for $0\lesssim\tilde{X}\leqslant 1$. This is to be compared to the result at low C where the advancing front was mainly located at $\tilde{X}\geqslant 1$. The density depletion is limited to the rear edge of the barrier $\tilde{X}\approx -1$, and the density is never lower than 0.5 the asymptotic value. The structure of the wake region does not show a strong scaling effect with Γ observed in Fig. 1(b), for the low C case. The scaled structure of the front region in terms of $\Gamma C(\tilde{X}-1)$ is presented in Fig. 4(a), and shows that the decay of the density is still well represented by the exponential form $A_-\exp(-\Gamma C\tilde{X})$ of the zeroth order mode, but with a Γ dependent amplitude A_-. The maximum amplitude of the wake, just behind the moving barrier seems to be similar for all the cases with large Γ, while the decay increases with Γ. The results in terms of the scaled distance $\Gamma C(\tilde{X}+1)$ may be compared to those in Fig. 2(b) for the slowly moving barrier, and we observe that the wake extends now further away from the barrier edge.

We now turn to the study of the local rescaled temperature[31] obtained from Eq. (34). The results for the $C=0.2$ case in Fig. 5 indicate that the shifting barrier produces a very strong heating of the system within the barrier, with maximum $T(\tilde{X})\approx 25T_o$ at the rear side of the barrier, in the region of lower density. At the scale of the maximum $T(\tilde{X})$, the temperature is apparently constant at the front side, but the inset shows that there is a sharp rise of temperature at $\tilde{X}\leqslant 1$, and also we observe a kind of precursor plateau over distances of the order $\tilde{X}\approx 20/\Gamma$ from the barrier edge, and with a Γ independent value $T(\tilde{X})/T_o\approx 1.5$. The width of that plateau may be understood from the huge enhancement of the density on the front side of the barrier, so that until the exponential decay makes $\Phi_0(1)\exp(-\Gamma C(\tilde{X}-1))\approx 1$, the large majority of the particles contributing to $\Phi_0(\tilde{X})$ belongs to the exponential component of that front, and the value of $T(\tilde{X})$ at the plateau would represent the temperature of the advancing front. The structure of $T(\tilde{X})$ of the wake is much narrower than at the front, and it indicates a moderate heating within the density depletion shown in Fig. 1.

In Fig. 6, we present the temperature distribution for the high velocity case, $C=2$, described in Figs. 3 and 4. The maximum temperature is $T(\tilde{X})\approx 5.5T_o$, and it is still located at the rear half of the barrier, associated with the minimum density. The "precursor film" at the front is much shorter and higher, so that only for the lowest value of Γ may be interpreted as an incipient "plateau," this is consistent with the interpretation given above when we consider the density distributions in Fig. 3. The most peculiar feature of $T(\tilde{X})$ at this high value of C is the appearance of local minimum between the main maximum and the front edge of the barrier. The relative importance of this feature increases with decreasing Γ, i.e., as the inertial effects become more important. A possible interpretation could be that the decrease in $T(\tilde{X})$ for $\tilde{X}\lesssim 1$ is a signature of the adiabatic expansion of the ideal fluid when it climbs the potential barrier. Therefore it should be restricted to large C and low Γ, to avoid the thermalization with the bath.

Finally, we present in Fig. 7 the results for the total force

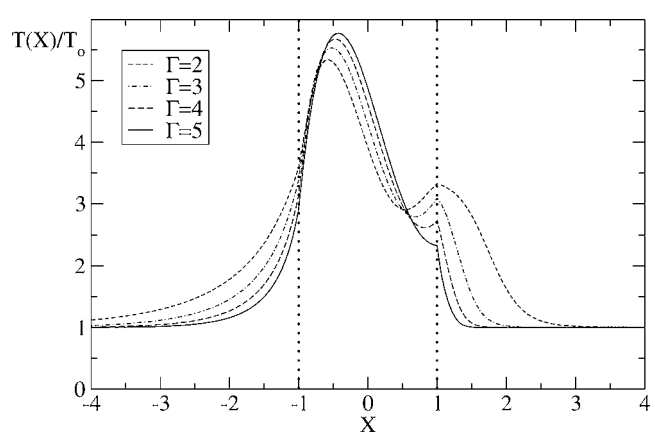

FIG. 6. Steady state temperature profile induced by a rapid drift, $C=2$, of the parabolic potential barrier. The position X is relative to the barrier and the vertical dotted lines are the barrier edges. Adimensional units [Eqs. (4) and (5)] are used for all the quantities.

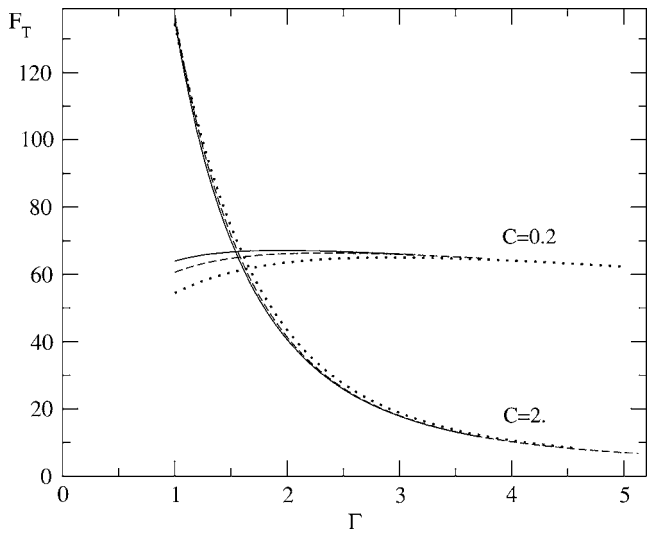

FIG. 7. Steady state total force exerted by the moving barrier on the particles for the shifting rates $C=0.2$ and $C=2$. The full lines are obtained using the expansion [Eq. (19)] in terms of the free modes up to $\mu_{\max}=4$, the dashed lines up to $\mu_{\max}=2$ and the dotted lines up to $\mu_{\max}=2$. Adimensional units [Eqs. (4) and (5)] are used for all the quantities.

F_T, from Eq. (33), obtained both for the low and high shifting rates, as functions of the damping Γ. We present the results for three different choices of the parametrization, $\mu_{\max}$ from 2 to 4, so that they give also a picture of the convergence of our treatment in terms of the free modes of the system. Notice that from Eqs. (33) and (35), the same results may be scaled to get the total power pumped by the barrier, and are directly associated with the excess of mass, and of kinetic energy through the relationship [Eq. (36)] imposed by the steady state condition. The results shows a clear difference between the $C=0.2$ case, with very little dependence of F_T on Γ, and the high rate shift, $C=2$, with a very rapid decay of the force for increasing damping.

V. CONCLUSIONS

Colloidal particles when subjected to external driving forces may exhibit properties which are different from those of the equilibrium systems. In the present paper, we have described the effect of a barrier moving at constant velocity in a one dimensional colloidal fluid in the approximation that the solvent is unaffected by the barrier. In contrast with previous approaches which have considered only overdamped dynamics, we have studied the case where inertia plays a role. The two major effects of inertial terms are first to determine the appearance of a wake structure, completely absent in the DDF treatment and of an infinite set of characteristic lengths in the regions near the moving barrier; and second to produce not only a strongly structured density distribution near the barrier, and the associated current density but also the higher order moments of the velocity distribution, which may be represented as a local temperature profile, very different from that of the thermalizing bath, and which shows interesting characteristics. It is also interesting that the method used here, based on the natural expansion of the distribution $P(X,V,\tau)$ for free systems, gives an intuitive connection with the previous results based on the DDF treatment, i.e., using the density distribution $\rho(X,\tau)=\rho_o\Phi_0(X,\tau)$ as the only relevant field. That approach is recovered in as the limit of the simplest description of $P(X,V,\tau)$ in terms of the first free mode (the only one with a purely diffusive dynamics, without an exponential decay time). The local balance of mass and force reproduce the DDF result of a Smoluchowski equation. To achieve the equivalent local balances for the energy, heat currents, etc., we have to enlarge the parametrization for $P(X,V,\tau)$, to include exponential decaying modes, which represent the effects of the inertial dynamics of the particles.

Here, we have analyzed only the simplest case, of one-dimensional spatial distributions in the dilute, ideal gas, limit. The equivalent results under other geometrical conditions, when the particles can bypass the moving barrier,[21,32] and including the effects of the particle interactions,[12,21] have been explored under the DDF assumptions, and it would be interesting to generalize them to the present approach.

It is perhaps worth to comment that the wake region is not specific to the flow of particles with inertia. Very similar effects were also found in higher dimensions for overdamped, Brownian particles driven past colloids, which act in this case as the potential barriers.[32] As shown by Penna *et al.*,[22] there exists a sum rule stating that the integral for the wake in any transversal plane to the direction of the drift vanishes, so that the depletion along the axis through the obstacle is exactly cancelled by the contribution from the lateral wings. Such a sum rule is valid in any dimension, but of course, in $D=1$ implies that there is no wake at all. The presence of a wake structure in $D=1$, in the inertial case, would correspond to a breaking of the sum rule for its transverse integral in $D>1$.

The present results perhaps are of relevance for microfluidic devices where colloidal particles move along narrow channels in order to understand what external forces are needed to induce a drift in the presence of Brownian fluctuations. The hydrodynamics interaction, which have been neglected here, could not be important in one dimension due to the screening effect, and we may expect that, at least at a qualitative level, the predictions made here could be accessible to experimental observation.

ACKNOWLEDGMENTS

P.T. acknowledges financial support from the Ministerio de Educacion y Ciencia of Spain, under Grant No. FIS2007-65869-C03-01, and the Comunidad Autonoma de Madrid, under Grant No. 0505/ESP-0299.

[1] T. M. Squires and S. R. Quake, Rev. Mod. Phys. **77**, 977 (2005).
[2] G. Whitesides and A. Stroock, Phys. Today **54**(6), 42 (2001).
[3] M. Gad-el'Hak, J. Fluids Eng. **121**, 5 (1999).
[4] C.-M. Ho and Y.-C. Tai, Annu. Rev. Fluid Mech. **30**, 579 (1998).
[5] P. Tabeling, *Introduction à la Microfluidique* (Belin, Paris, 2003).
[6] H. Gau, S. Herminghaus, P. Lenz, and R. Lipowsky, Science **283**, 46 (1999).
[7] R. F. Service, Science **282**, 399 (1998).
[8] A. Terray, J. Oakey, and D. W. M. Marr, Science **296**, 1841 (2002).
[9] B. Cui, H. Diamant, and B. Lin, Phys. Rev. Lett. **89**, 188302 (2002).
[10] M. Sullivan, K. Zhao, C. Harrison, R. H. Austin, M. Megens, A. Hollingsworth, W. B. Russel, Z. Cheng, T. Mason, and P. M. Chaikin, J. Phys.: Condens. Matter **15**, S11 (2003).

[11] C. Bechinger, J. Phys.: Condens. Matter **13**, R321 (2001).
[12] F. Penna and P. Tarazona, J. Chem. Phys. **119**, 1766 (2003).
[13] U. Marini Bettolo Marconi and P. Tarazona, J. Chem. Phys. **110**, 8032 (1999); J. Phys.: Condens. Matter **12**, A413 (2000).
[14] A. J. Archer and R. Evans, J. Chem. Phys. **121**, 4246 (2004).
[15] A. Yoshimori, Phys. Rev. E **59**, 6535 (1999).
[16] R. Evans, Adv. Phys. **28**, 143 (1979).
[17] U. Marini Bettolo Marconi and P. Tarazona, J. Chem. Phys. **124**, 164901 (2006).
[18] H. A. Kramers, Physica (Amsterdam) **7**, 284 (1940).
[19] U. Marini Bettolo Marconi and S. Melchionna, J. Chem. Phys. **126**, 184109 (2007).
[20] U. Marini Bettolo Marconi, P. Tarazona, and F. Cecconi, J. Chem. Phys. **126**, 164904 (2007).
[21] J. Dzubiella and C. N. Likos, J. Phys.: Condens. Matter **15**, L147 (2003).
[22] F. Penna, J. Dzubiella, and P. Tarazona, Phys. Rev. E **68**, 061407 (2003).
[23] R. Pagnani, U. Marini Bettolo Marconi, and A. Puglisi, Phys. Rev. E **66**, 051304 (2002).
[24] F. Cecconi, F. Diotallevi, U. M. B. Marconi, and A. Puglisi, J. Chem. Phys. **120**, 35 (2004); **121**, 5125 (2004).
[25] H. Risken, *The Fokker-Planck Equation* (Springer-Verlag, Berlin, 1984).
[26] C. Gardiner, *Handbook of Stochastic Methods for Physics, Chemistry and in the Natural Sciences* (Springer-Verlag, Berlin, 1994).
[27] P. Reimann, C. van der Broeck, H. Linke, P. Hanggi, J. M. Rubi, and A. Perez-Madrid, Phys. Rev. Lett. **87**, 010602 (2001).
[28] M. Borromeo and F. Marchesoni, Phys. Lett. A **249**, 199 (1998).
[29] M. Rex, H. Lwen, and C. N. Likos, Phys. Rev. E **72**, 021404 (2005).
[30] M. von Smoluchowski, Ann. Phys. **48**, 1103 (1916).
[31] C. Lopez and U. Marini Bettolo Marconi, Phys. Rev. E **75**, 021101 (2007).
[32] J. Dzubiella, H. Lowen, and C. N. Likos, Phys. Rev. Lett. **91**, 248301 (2003).